Shao *et al. Journal of Translational Medicine* (2024) 22:996
https://doi.org/10.1186/s12967-024-05792-6

Journal of
Translational Medicine

RESEARCH Open Access

Implementing an intelligent diagnosis and treatment system for in-hospital cardiac arrest in the Utstein style: a multi-center case study

Yan Shao[1], Zhou Yang[2], Wei Chen[2] and Yingqi Zhang[1*]

Abstract

Background Cardiac arrest presents a variety of causes and complexities, making it challenging to develop targeted treatment plans. Often, the original data are either inadequate or lack essential patient information. In this study, we introduce an intelligent system for diagnosing and treating in-hospital cardiac arrest (IHCA), aimed at improving the success rate of cardiopulmonary resuscitation and restoring spontaneous circulation.

Methods To compensate for insufficient or incomplete data, a hybrid mega trend diffusion method was used to generate virtual samples, enhancing system performance. The core of the system is a modified episodic deep reinforcement learning module, which facilitates the diagnosis and treatment process while improving sample efficiency. Uncertainty analysis was performed using Monte Carlo simulations, and dependencies between different parameters were assessed using regular vine copula. The system's effectiveness was evaluated using ten years of data from Utstein-style IHCA registries across seven hospitals in China's Hebei Province.

Results The system demonstrated improved performance compared to other models, particularly in scenarios with inadequate data or missing patient information. The average reward scores in two key stages increased by 2.3–9 and 9.9–23, respectively.

Conclusions The intelligent diagnosis and treatment effectively addresses IHCA, providing reliable diagnosis and treatment plans in IHCA scenarios. Moreover, it can effectively induce cardiopulmonary resuscitation and restoration of spontaneous circulation processes even when original data are insufficient or basic patient information is missing.

Keywords In-hospital cardiac arrest, Intelligent diagnosis and treatment system, Hybrid mega trend diffusion, Modified episodic deep reinforcement learning, Uncertainty analysis

*Correspondence:
Yingqi Zhang
zhangyingqi@hebmu.edu.cn
[1] Department of Emergency, The First Hospital of Hebei Medical University, Shijiazhuang, China
[2] System Integration Center, China Mobile Communication Group Hebei Co., LTD., Shijiazhuang, China

Background

Cardiac arrest (CA) is a common critical occurrence in the emergency room and has become a significant public health concern due to its high mortality rate [1]. CA management involves cardiopulmonary resuscitation (CPR) and restoration of spontaneous circulation (ROSC). CA can be divided into two types based on the patient's hospitalization status at onset: in-hospital CA (IHCA) and out-of-hospital CA (OHCA). The pathogenesis of the two types of CA is essentially the same, and different treatments are sometimes used only because of the availability of medical equipment in different settings. Rapid diagnosis and treatment are required to treat CA; however, basic patient information is usually insufficient or missing. Currently, CA treatment relies mainly on the subjective experience of doctors, which can result in misdiagnosis [2]. To improve CA treatment, many researchers have analyzed and studied it in various ways, providing important references for CA treatment development.

Abrams et al. [3] and Kumar et al. [4] used extracorporeal CPR to replace traditional CPR for IHCA treatment and found that it effectively improved survival rates. Girotra et al. [5] proposed post-resuscitation care for IHCA and achieved good results. Neurological complications of IHCA [6], induced consciousness cure methods [7], and airway management methods [8] have also been reported. These CA diagnosis and treatment methods have many advantages; however, they all depend on the subjective experience of doctors, which can easily lead to misdiagnoses.

Artificial intelligence (AI) development and the combination of AI elements with medical research have received increased attention from many researchers [9] for applications such as drug design [10], cardiovascular medicine [11], and cancer research [12]. Compared to traditional methods, AI technology can treat and diagnose complex diseases more objectively. Therefore, applying AI technology for IHCA can produce more rapid and accurate diagnosis and treatment results [13]. Previous studies have used AI methods to analyze CA from various perspectives. However, current research focuses on the analysis [14], summary [15], and discussion of relevant data [16, 17], and few researchers have considered how to improve and innovate CA treatments. Therefore, the development of improved treatment methods for CA is a priority.

Relative to other AI methods, deep reinforcement learning (DRL) combines the strong sequential decision-making ability of reinforcement learning (RL) with the superior perception ability of deep learning (DL) [18, 19] and uses a statistical model that can more effectively complete CA's dynamic diagnosis and treatment process. However, there are three major obstacles to using DRL for diagnosis and treatment. First, training a well-performing DRL model requires large amounts of original data. When a trained model is used for diagnosis, complete basic patient information is required to obtain accurate results. However, it is often impossible to obtain sufficient original data to complete model training. Furthermore, owing to the abrupt nature of IHCA, interventions must often be initiated before complete data are available.

Virtual sample technology provides an effective method of solving these problems. The most popular virtual sample technology is mega trend diffusion (MTD); however, it describes all data with only one type of distribution, which is too simple to reflect the characteristics of the data accurately [20]. Dong et al. [21] used a double-distribution MTD to generate virtual samples; that is, a uniform distribution was used to describe the original sample interval, and a triangular distribution was used to describe the virtual sample interval, further improving performance. However, the virtual sample interval is complex; hence, further division is required.

Second, DRL is commonly applied to virtual rather than real-world tasks because of its low sample efficiency. Therefore, solving the problem of low sample efficiency is key to completing diagnosis and treatment system modeling with DRL [22]. The traditional method for improving sample efficiency is to use episodic memory to build an episodic DRL. Min et al. [23] and Nishio et al. [24] proposed a model-free episodic control and neural episodic control (two episodic DRL models) to remember the best decision information, which can assist the agent in choosing the best action faster and reduce the required sample numbers. The former has a fast update speed but insufficient stability, whereas the latter has good stability but a slow speed. Hence, the proposed modified episodic DRL model combines the advantages of fast update speed and good stability, significantly improving the results.

Third, strong uncertainty regarding IHCA treatment is likely due to the numerous causes and complexities of IHCA. Hence, a reasonable uncertainty analysis of diagnosis and treatment processes is essential. The Monte Carlo simulation (MCS) is a commonly used method. Many basic parameters should be considered, such as the initial heart rhythm, systolic pressure, and body temperature. Parameters do not exist alone; therefore, it is necessary to consider their interdependence. The regular vine copula (RVC) is the most effective method for constructing dependencies among complex high-dimensional parameters [25]. Hence, MCS and RVC should be combined to generate more accurate analysis results.

In this study, an intelligent DRL-based diagnosis and treatment system for IHCA was developed using the Utstein style. According to the registration content of IHCA under the Utstein mode, a hybrid MTD (HMTD) was used to construct a virtual sample to improve the system performance when original data were insufficient or basic patient information was missing. Subsequently, the modified episodic DRL (MEDRL) was used to develop an intelligent diagnosis and treatment system for CPR and ROSC based on the basic situation of different cases during IHCA to maximize CPR success rates and maintain optimal blood pressure during ROSC. The sample efficiency was effectively promoted by improving the episodic memory-updating method and experience replay memory. Furthermore, uncertainty analysis was conducted using MCS, and the dependency between the uncertainty analyses of different parameters was determined using RVC. To the best of our knowledge, this is the first study to build an intelligent diagnosis and treatment system for IHCA and to use AI to complete a specific treatment.

Methods

Data sources

Data were obtained from the IHCA and CPR registration networks of the emergency intelligence platform of the China Hebei Emergency Technology Innovation Center (ETIC). Ten years of data from seven hospitals were included in this study. Registry data collection was based on the Utstein mode of the IHCA and CPR registration forms, which mainly included the annual number of emergency department visits, general condition, conditions during IHCA and CPR, ROSC, ROSC to hospitalization, hospitalization to discharge, and follow-up after discharge. The study was approved by the China Hebei ETIC, Hebei, China (approval number: 20221015). Written informed consent was obtained from all patients.

Hybrid mega trend diffusion (HMTD)

The basic structure of an HMTD is illustrated in Fig. 1, where [L, R] denotes the original sample interval. Using basic MTD principles and original data, the extended sample intervals [A, L] and [R, B] are estimated, enabling virtual sample calculation. The basic MTD principles and the virtual sample generation process have been described in previous studies [21, 26]. This section focuses on using different distributions to complete the sample extension based on traditional MTD. Virtual samples can be generated in the original sample interval ([L, R], called interval 1) and in two sample expansion intervals ([A, L] and [R, B], called intervals 2 and 3, respectively). For a traditional MTD, virtual samples in all three intervals are assumed to follow a normal distribution. In HMTD, a normal distribution is still used for interval 1 due to the numerous original samples in this region. Compared with the newly generated virtual samples, the original samples account for the majority; thus, it is assumed they conform to a normal distribution. In the two extended intervals, where the area of interval 1 is larger than that of interval 2, a uniform distribution is used for interval 1, while a triangular distribution is used for interval 2. Thus, HMTD uses appropriate distributions to describe different intervals based on their respective characteristics, effectively avoiding imbalanced distribution and inaccurate feature characterization of samples.

$$A = \begin{cases} Cen + Skew_A \cdot \sqrt{-2 \cdot \frac{v^2}{S_A In(10^{-20})}} & A < L \\ L & A > L \end{cases} \tag{1}$$

$$B = \begin{cases} Cen + Skew_B \cdot \sqrt{-2 \cdot \frac{v^2}{S_B In(10^{-20})}} & B > R \\ R & B < R \end{cases} \tag{2}$$

$$Skew_A = \frac{S_A}{SA + S_B}, Skew_B = \frac{S_B}{SA + S_B}, Cen = \frac{Max + Min}{2} \tag{3}$$

where *Cen* is the sample set center point, v^2 is the variance, S_A and S_B are the number of samples smaller and greater than *Cen*, respectively; $Skew_A$ and $Skew_B$ are the left and right diffusion skewness, respectively.

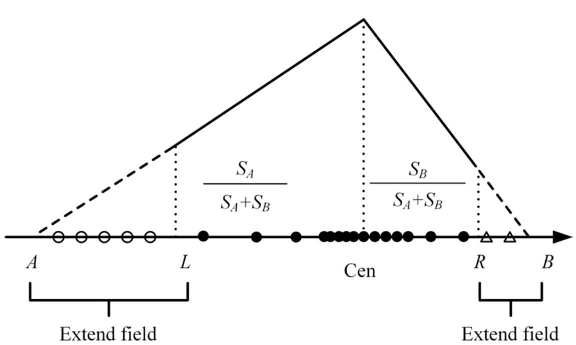

Fig. 1 Structure diagram of hybrid mega trend diffusion. Where *Cen* is the sample set center point, v^2 is the variance, S_A and S_B are the number of samples smaller and greater than *Cen*, respectively; $Skew_A$ and $Skew_B$ are the left and right diffusion skewness, respectively

The MEDRL diagnosis and intelligent treatment system

Agent, environment, state, action, and reward are the five key elements of DRL. Each time, the agent receives the current state information (s_t) from the environment and chooses and executes the optimal action (a_t). There is a reward (r_t) response from the environment to the agent, and the environment transitions to the next state (s_{t+1}). Therefore, a DRL sample is $Sample_t = (s_t, a_t, r_t, s_{t+1})$. [27] To solve the problem of low sample efficiency in DRL, an MEDRL model that combines the advantages of fast update speed and good stability is proposed in this section. This is achieved by improving the episodic memory-updating method and experience replay memory.

Experience replay memory

In traditional DRL, only one experience replay memory (ERM) is used. To achieve better memory performance, a peak-end rule was introduced by applying two ERMs. One is the same as the traditional ERM, and another, called "Highmemory," is used only to store episodes in which the reward exceeds the previous best. Although these two ERMs offer better sample efficiency than traditional methods, there remains a problem of insufficient sample diversity. [28]

In this study, we propose a percentile optimum ERM (POERM) to replace Highmemory. During the operation, a dynamic episode storage method is used; that is, when each episode ends, all the episode data are stored in the POERM if the total episode rewards R_{et} were equal to or greater than the threshold value (R_{th}). The threshold value can be generated as follows:

The total episode rewards and dynamic threshold values are calculated at the end of each episode as follows:

$$R_{et} = \sum_{t=1}^{N} r_t \tag{4}$$

$$R_{th} = f(R_p, y_{\text{percen}}) \tag{5}$$

where r_t is the reward at each time point, R_p is the total reward sequence of the last K episodes, and y_{percen} is the percentile that constantly changes with the training progress. The larger the y_{percen}, the greater the R_{th}, but the worse the sample diversity. To ensure both stability and diversity, the initial y_{percen} value was set to 75% and gradually increased (Fig. 2). This process increases sample diversity while ensuring stability.

During training, the following method was used to sample episode data from the two ERMs:

$$\text{Sample} = \begin{cases} [S_{ERM}\left((1-\alpha)*y\right), S_{\text{percen}}(\alpha*y)],\ if\ p < p_{th} \\ S_{ERM}\left(y\right), otherwise \end{cases} \tag{6}$$

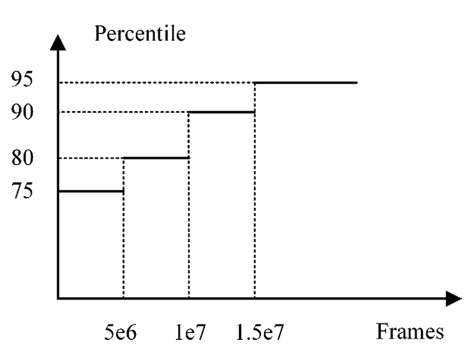

Fig. 2 Dynamic percentile changing diagram

where y is the amount of the sample, $\alpha \in [0,1]$ is the proportion sampled from the two ERMs, and $S_{\text{ERM}}\left((1-\alpha)*y\right)$ and $S_{\text{percen}}\left(\alpha*y\right)$ denote that there are $\lfloor(1-\alpha)*y\rfloor$ and $\lfloor\alpha*y\rfloor$ samples randomly sampled from the two ERMs.p is the triggering probability between the traditional and two ERMs models. Only when p is smaller than the threshold (p_{th}) will the two ERM model be triggered.

Episodic memory updating

The episodic value Q^{n}_{Ep} of all state-action pairs can be calculated as follows:

$$Q^{n}_{Ep}(s_j, a_j) = \sum_{j=1}^{N} \gamma^{j-1} r_j \tag{7}$$

where N is the length of episode, γ^{j-1} is the discount rate, which $\in [0,1]$.

If the state-action pair of the new episodic value Q^{n}_{Ep} is not stored in the ERM, it will be added directly. If the state-action pair already exists, then the newly calculated episodic value ($Q^{n}_{\text{Ep}}(s_j, a_j)$) and the original episodic value ($Q_{\text{Ep}}(s_j, a_j)$) will be compared. If $Q^{n}_{\text{Ep}}(s_j, a_j)$>$Q_{\text{E}}(s_t, a_t)$, the episodic memory will be updated, and $Q^{n}_{\text{Ep}}(s_j, a_j)$ replaces the original value to be stored.

The above method can improve episodic memory-updating speed; however, it may lack stability when the updating speed is too high. To solve this, we ameliorated the updating mode, which can be expressed as:

$$Q_{\text{Ep}}(s_j, a_j) = Q_{\text{Ep}}(s_j, a_j) + \beta(Q^{n}_{\text{Ep}}(s_j, a_j) - Q_{\text{Ep}}(s_j, a_j)) \tag{8}$$

Stable updating can be effectively achieved by controlling the learning rate, β.

In some complex cases, the agent requires considerable time to complete the full-episode interaction; therefore, the update frequency is low, and the $Q_{\text{Ep}}(s_j, a_j)$ has poor timeliness. We use the k-step estimation method, which uses the K step estimated value to replace the $Q^{n}_{\text{Ep}}(s_j, a_j)$ in (8) when the number of steps that the agent needs to perform in each episode is greater than K:

$$Q^{new}_{EP}(s_t, a_t) = \sum_{l=1}^{K} \gamma^{j-1} r_l + \gamma^{K} \max_{\mu\prime} Q_t(s_{t+K}, \mu\prime) \tag{9}$$

where $Q_t(s_{t+K}, \mu\prime)$ is the weighted sum of the output value $Q(s_{t+K}, \mu\prime|\theta^{T})$ from the DQN target network and $Q_{\text{Ep}}(s_t, \mu\prime)$ from episodic memory:

$$Q_t(s_{t+K}, \mu\prime) = \begin{cases} Q(s_{t+K}, \mu\prime|\theta^{T}), if\,(s_{t+K}, \mu\prime) \notin Q_{Ep} \\ \varepsilon Q\left(s_{t+K}, \mu\prime|\theta^{T}\right) + (1-\varepsilon) Q_{Ep}(s_t, \mu\prime), otherwise \end{cases} \tag{10}$$

where $\varepsilon \in [0,1]$.

Finally, the modified episodic memory updating manner was:

$$Q_E(s_t,a_t) = \begin{cases} Q_{EP}^{new}(s_t,a_t), if\, (s_t,a_t) \notin Q_E \\ Q_{EP}(s_t,a_t) + \beta(Q_{EP}^{new}(s_t,a_t) - Q_{PE}(s_t,a_t)), if Q_{EP}^{new}(s_t,a_t) > Q_{EP}(s_t,a_t) \end{cases} \tag{11}$$

where $Q_{EP}^{new}(s_t,a_t)$ can be get through (9) and (10).

Diagnosis and intelligent treatment system

The basic structure of the intelligent diagnosis and treatment system is illustrated in Fig. 3.

For Stage 1, the treatment time was set to 60 min, and the time step was set to 2 min. During this interval, DRL assesses the current state, executes the corresponding action, and transfers the action to the next state. The state space of Stage 1 was the systolic pressure value at time *t*, and the action space included chest compressions, adrenaline (epinephrine) injections, electrical defibrillation, and initiation or termination of tracheal intubation. Under certain basic conditions (age, sex, IHCA causes, initial heart rhythm, and presence of an underlying disease), an intelligent diagnosis and treatment system was used to establish a stepwise diagnosis and treatment. If the basic patient information is insufficient or missing at this stage, with scarce information as input, the training process of the system can still be achieved through the strong perceptual ability and robustness of the deep neural network. Successful resuscitation cases in the data were used as the standard treatment method in the same situation, and the similarities between the treatment plan proposed by the intelligent diagnosis and treatment system and the standard treatment method were compared. The following four comparisons were made: (1) whether chest compression was performed, (2) whether adrenaline was injected and the dose was consistent, (3) whether electric defibrillation was performed, and (4) whether tracheal intubation was performed. The reward was 100 for consistency and 0 for inconsistency. The reward was counted for 60 min throughout the resuscitation process. The objective function of Stage 1 is to achieve a systolic pressure greater than zero. When the systolic pressure was greater than zero, the CPR process was considered successful, and Stage 2 was initiated. Resuscitation was considered to have failed if the systolic pressure remained at zero until the end of the treatment period (60 min).

For Stage 2, the treatment time was set to 24 h, and the time step was set to 30 min. During this interval, DRL assesses the current state, executes the

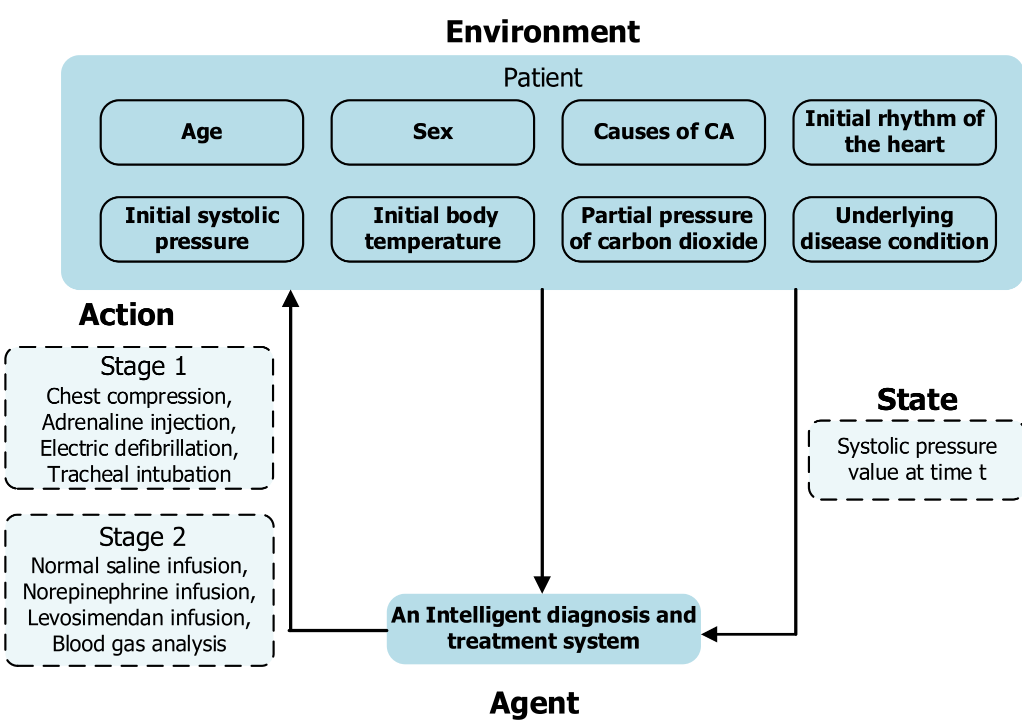

Fig. 3 Basic structure of the intelligent diagnosis and treatment system

corresponding action, and transfers the action to the next state. The state space of Stage 2 was also the systolic pressure value at time *t*, and the action space included normal saline infusion, noradrenaline infusion, levosimendan infusion, and blood gas analysis. Using 90 mmHg as the standard systolic blood pressure, the objective function of Stage 2 was to achieve a systolic pressure of 90 mmHg, and the allowable error was ± 10 mmHg. From the onset of ROSC and under certain basic conditions (such as age, sex, partial pressure of carbon dioxide, initial systolic pressure, initial body temperature, and presence of an underlying disease), an intelligent diagnosis and treatment system was used to establish stepwise diagnosis and treatment, and the reward *(R)* for each step was obtained according to the reference data as follows:

$$R = \begin{cases} T - |X-90| & X \leq 90 \\ T & X > 90 \end{cases} \tag{12}$$

where T is a constant, and X is the systolic pressure at the current moment. When $X \leq 90$, the closer the systolic pressure to the standard value, the larger the reward. When $X > 90$, the rewardwas maintained at T.

If the patient's basic information was insufficient or missing at this stage, the solution would be the same as in Stage 1.

The constraints of both stages include:

$$100/\text{min} \leq f_c \leq 120/\text{min}, \tag{13}$$

$$0.5\text{mg} \leq H_e \leq 1\text{mg}, \tag{14}$$

$$2\text{min} \leq I_e \leq 10\text{min}, \tag{15}$$

$$I_D \geq 2\ \text{min}, \tag{16}$$

$$H_s \leq 800\text{mL}, \tag{17}$$

$$0.1\mu\text{g/kg/min} \leq H_N \leq 2\text{mg/kg/min}, \tag{18}$$

$$0.05\mu\text{g/kg/min} \leq H_L \leq 2\text{mg/kg/min}, \tag{19}$$

$$0.5\text{hour} \leq I_b \leq 5\text{hour}, \tag{20}$$

where f_c is the frequency of chest compressions, H_e is a single dose of adrenaline injection,I_e is the interval between adrenaline injections, I_D is the interval between electrical defibrillations, H_s is the total dose of normal saline infusion, H_N is a single dose of noradrenaline infusion, H_L is a single dose of levosimendan infusion, and I_b is the interval for blood gas analysis.

Uncertainty analysis

The strong uncertainty associated with IHCA treatment likely results from its numerous causes and complexities. To address this, stochastic scenarios were generated using MCS to analyze the uncertainties, and RVC was used to construct dependencies among all basic parameters.

The stochastic scenario generation method has been described in previous studies [29, 30]. To minimize the uncertainty of the diagnosis and treatment processes, two action spaces were used to derive a finite set of scenarios (M) for each time period through MCS. Each scenario denoted as $\omega_i \in M$, comprises variables with uncertainties.

$$\omega_i = \left\{A_1^{\omega_i}(t),\ A_2^{\omega_i}(t)\right\} \tag{21}$$

where $A_1^{\omega}(t)$ and $A_2^{\omega}(t)$ are action spaces of Stages 1 and 2, respectively (the detailed description is included in the DRL intelligent diagnosis and treatment system section). The marginal probability density function (MPDF) of each scenario was calculated using a Gaussian mixture model. [31]

$$P(\omega_i) = \{P(\omega_1), P(\omega_2), \cdots, P(\omega_n)\}^T = H(\omega_i|\theta_i) \tag{22}$$

where H $(\cdot)$ is the Gaussian mixture function, and θ_I is the parameter set of each scenario.

After the MPDF was generated, the dependence structures of all basic parameters were constructed using RVC. The joint PDF of all the basic parameters was calculated as follows:

$$P = C(P(\omega_1),\ P(\omega_2), \cdots, P(\omega_n)) \tag{23}$$

The RVC modeling process mainly contains two parts: [32]

1. Selecting the suitable regular vine structure and determining the set of all edges.
2. Choosing a criterion to select the best goodness-of-fit binary *copula* module for each edge and optimizing its parameters.

The Akaike information criterion was chosen for the goodness-of-fit in this study. After generating the MPDF through MCS and constructing the dependency structures using RVC, the joint PDF was obtained by combining both, yielding the uncertainty analysis results.

Statistical analysis

All statistical analyses were performed using SPSS version 25.0 (IBM Corp., Armonk, NY, USA). The data used for each experiment were randomly selected, and the results were obtained by repeatedly calculating the average values under the same circumstances. The Mann–Whitney U test was used to compare differences between groups. Data are presented as skewed distributions or numbers (%) depending on the data distribution. Statistical significance was set at a p-value of less than 0.05.

Results

Patients' basic characteristics

Data from the IHCA and CPR registration networks of the ETIC were used as treatment references, and basic information regarding the CPR and ROSC treatments are presented in Tables 1 and 2, respectively.

As shown in Table 1, younger patients had a lower incidence of underlying diseases and a higher incidence of successful resuscitation. The probability of IHCA occurrence was much greater in men than in women, and the probability of cardiogenic IHCA was higher than that of non-cardiac IHCA. The earlier the four main treatment modalities began (chest compressions, adrenaline injection, electric defibrillation, and tracheal intubation), the greater the chance of resuscitation. Among the airway management strategies, there was no notable difference

Table 1 Basic parameters of the resuscitation process

Parameter	Total (n = 7,790)	Resuscitation success (n = 1,350)	Resuscitation failure (n = 6,440)	p-value[c]
Age[a], years	66 (55, 77)	65 (55, 76)	67 (56, 77)	0.03
Sex[b] (n, %)				
Male	5350 (68.68)	990 (73.33)	4360 (67.70)	0.025
Female	2440 (31.32)	360 (26.67)	2080 (32.30)	0.025
Causes of IHCA[b] (n, %)				
Cardiogenic	3550 (45.57)	390 (28.89)	3160 (49.07)	< 0.01
Non-cardiac	2720 (34.92)	550 (40.74)	2170 (33.70)	< 0.01
Unknown	1520 (19.51)	410 (30.37)	1110 (17.23)	< 0.01
Initial rhythm of the heart (n, %)				
Asystole	2850 (36.59)	430 (31.58)	2420 (37.58)	0.025
Pulseless electrical activity	920 (11.81)	120 (8.89)	800 (12.42)	0.32
Ventricular fibrillation	430 (5.52)	80 (5.93)	350 (5.43)	0.02
Pulseless ventricular tachycardia	100 (1.28)	20 (1.48)	80 (1.24)	0.04
Bradycardia	650 (8.34)	190 (14.07)	460 (7.14)	0.01
Unknown	2840 (36.46)	510 (37.78)	2330 (36.18)	0.03
Chest compression start time (min)	0.5 (0, 1.5)	0.5 (0, 1)	1 (0, 2)	0.01
Chest compression total duration (min)	30 (8, 70)	12 (5, 25)	50 (27, 79)	0.01
Airway management start time (min)	15 (10, 25)	8 (5, 17)	20 (12, 30)	0.01
Airway management strategies (n, %)				
Endotracheal intubation	5200 (66.75)	895 (66.30)	4305 (66.85)	< 0.01
Cuffed oropharyngeal airway	90 (1.16)	20 (1.48)	70 (1.09)	< 0.01
Supraglottic airway	10 (0.13)	0 (0.00)	10 (0.16)	< 0.01
Tracheotomy	110 (1.41)	30 (2.22)	80 (1.24)	0.63
Mask	230 (2.95)	35 (2.59)	195 (3.02)	0.01
No advanced airway	2150 (27.60)	370 (27.41)	1780 (27.64)	0.04
CPR total duration[a] (min)	47.00 (23.00, 80.00)	15.00 (8.00, 30.00)	55.00 (30.00, 86.25)	< 0.01
Time to first administration of adrenaline (s)	87.00 (20.00, 759.50)	54.00 (16.00, 296.50)	100 (21.00, 864.00)	0.01
Single dose of adrenaline injection[a] (mg)	9.00 (2.00, 20.00)	3.00 (1.00, 6.00)	10.00 (4.00, 20.00)	< 0.01
Number of adrenaline injections (n)	15 (7, 25)	5 (3, 10)	17 (10, 28)	0.01
Number of electric defibrillation[b] (n)	6 (2, 10)	3 (1, 5)	5 (3, 10)	< 0.01
Electric defibrillations start time (min)	0.5 (0, 2)	0.5 (0, 1.5)	1 (0, 2)	0.01

[a] Parameters such as age, a single dose of adrenaline, and cardiopulmonary resuscitation start time are presented as skewed distributions M (P_{25}, P_{75}), where M is the median and P_{25} and P_{75} are both quartiles

[b] Other parameters such as sex, causes of cardiac arrest, and defibrillation are presented as numbers (n) and percentages (%)

[c] The level of statistical significance was set at p < 0.05

Table 2 Basic information of the ROSC treatment process

Parameter	Total (n = 1350)	ROSC success (n = 230)	ROSC failure (n = 1120)	p-value
Age, years	65 (55, 76)	63 (54, 75)	67 (57, 77)	0.01
Sex (n, %)				
Male	990 (73.33)	157 (68.26)	833 (74.38)	< 0.01
Female	360 (26.67)	73 (31.74)	287 (25.62)	< 0.01
Initial systolic pressure (mmHg)	75 (50, 90)	75 (60, 95)	70 (50, 80)	0.01
Initial body temperature	37.3 (36.0, 39.0)	37.0 (36.2, 39.0)	37.5 (36.0, 39.1)	0.04
Partial pressure of carbon dioxide (mmHg)	50 (38, 75)	45 (35, 60)	55 (50, 80)	0.03
Finger pulse oxygen (%)	98 (93, 100)	99 (95, 100)	95 (90, 96)	0.01
Underlying disease (n, %)				
No underlying disease	128 (9.48)	61 (26.52)	67 (5.98)	< 0.01
Single underlying disease	506 (37.48)	57 (24.78)	449 (40.09)	0.03
More than one underlying disease	395 (29.26)	49 (21.31)	346 (30.89)	< 0.01
Unknown	321 (23.78)	63 (27.39)	258 (23.04)	0.025
Volume of normal saline infusion (mL)	2000 (1000, 3000)	2500 (1000, 3500)	1500 (1000, 2000)	< 0.01
Noradrenaline infusion pump speed (μg/kg/min)	0.5 (0.1, 1.5)	0.3 (0, 1.2)	0.8 (0.5, 1.7)	0.32
Levosimendan infusion pump speed (μg/kg/min)	0.1 (0, 0.16)	0.09 (0, 0.15)	0.12 (0, 0.18)	0.02
Interval for blood gas analysis (hour)	1 (0.5, 2)	1.5 (1, 2.5)	1 (0.5, 1.5)	0.01

ROSC restoration of spontaneous circulation

in successful resuscitation rates between patients with tracheal intubation and those with masks. The total duration of CPR was shorter, and the total dose of adrenaline was lower in the successful resuscitation group than in the death group, which is generally consistent with the actual clinical results.

Table 2 shows that age, sex, and IHCA cause had no significant effects on the success of ROSC; however, body temperature, systolic pressure, and respiratory conditions did. An increase in the body temperature of the patient after resuscitation indicated that the degree of brain injury was serious. Even if resuscitation was successful, maintaining circulatory stability remained difficult, which occasionally led to ROSC failure.

Based on the analysis of Tables 1 and 2, three different models (DRL-MCS, RL-MCS, and DRL without MCS) were used for the intelligent diagnosis and treatment of IHCA.

Performance evaluation of the MEDRL model

The MEDRL is used to improve sample efficiency by ameliorating episodic memory-updating and ERM. To demonstrate this superiority, two benchmark models—EDRL and traditional DRL (without episodic memory)—and a novel model—multiple episodic memory DRL (Multi-EMDRL)—were used. [33] A comparison of the results is shown in Figs. 4 and 5 and Table 3. A model with higher sample efficiency means that, under the same training conditions, it can obtain the same reward using fewer samples or obtain a higher score using the same sample.

We randomly chose three games from the OpenAI Gym to test the performance of the three different models. To increase the accuracy of the comparison, each game was run 10 times, and the average reward was calculated (Fig. 4, Table 3). We found that, compared with two benchmark models, the proposed MEDRL could obtain the highest reward using the same number of samples. As a novel six-layer hybrid model, the MEMDRL model obtains results almost equivalent to those of the proposed model. However, the Multi-MEDRL has a more complex structure (with three episodic memory modules), and thus, the sample efficiency of Multi-MEDRL is poor.

Furthermore, the comparison result of the game "Pong" is shown in Fig. 5. This shows that to achieve the same reward, MEDRL needed only 4.5 million frames, whereas EDRL and DRL needed 8.75 and 9.5 million frames, respectively. The novel Multi-MEDRL model, owing to its complex structure, needs 9.75 million frames.

Diagnosis and treatment performance of different models

To verify the effectiveness of the MEDRL-MCS-RVC model, three other models were used for comparison and verification: MEDRL-MCS (without dependency), MEDRL (without uncertainty analysis), and mixed-integer nonlinear programming (MINLP).

The two-stage treatment total reward for a randomly selected case from each of the seven hospitals under the different models is shown in Figs. 6 and 7. The figures show that the first stage of the treatment process (CPR

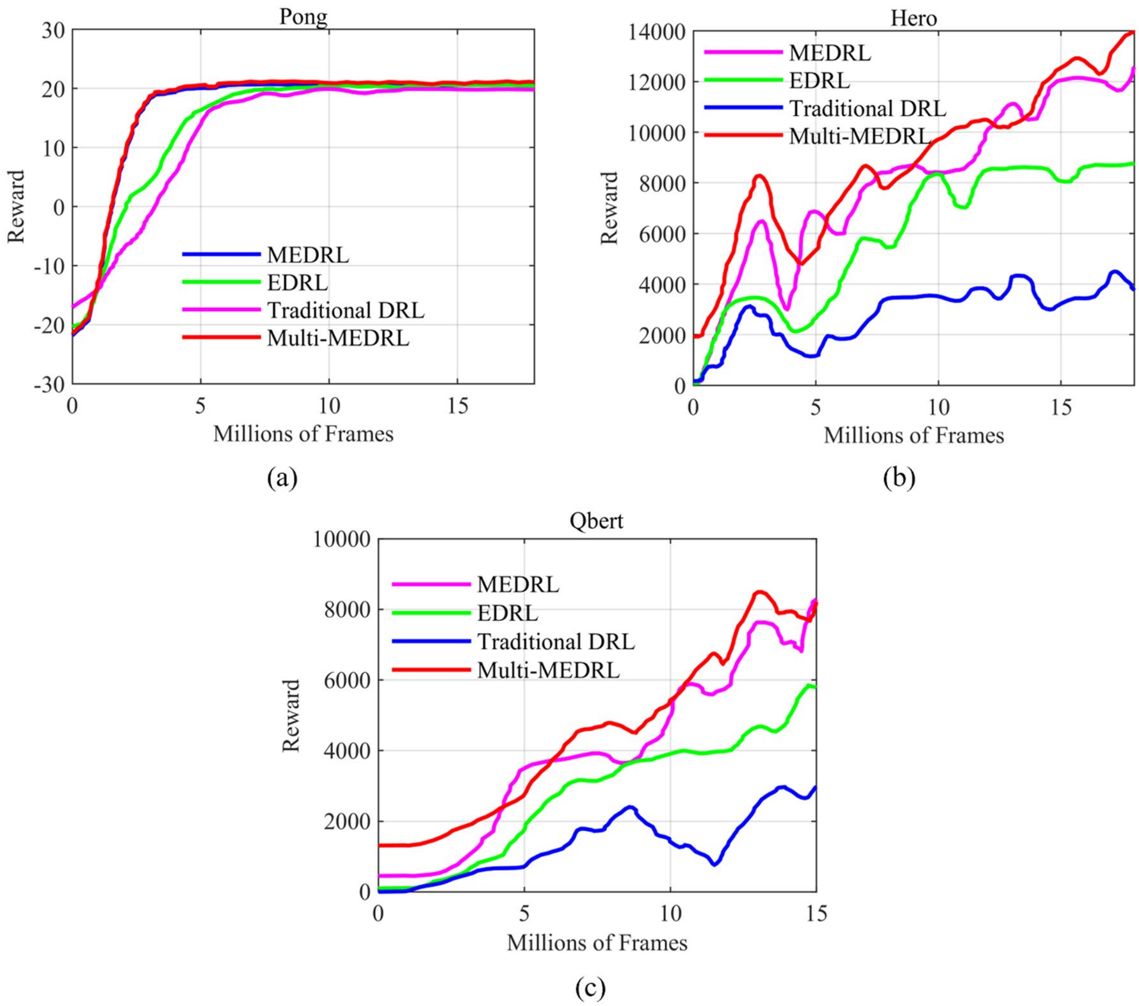

Fig. 4 Performance of different models on three randomly selected games. *DRL* deep reinforcement learning, *EDRL* episodic deep reinforcement learning, *MEDRL* modified episodic deep reinforcement learning

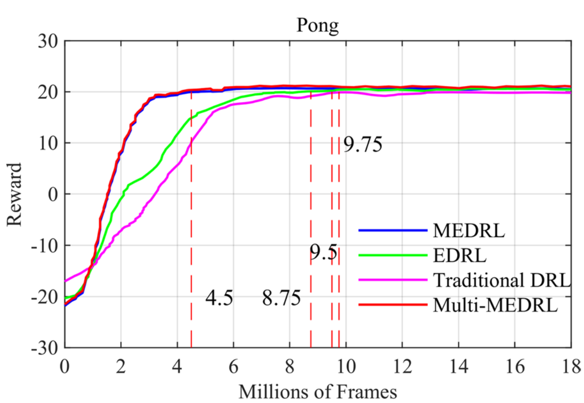

Fig. 5 Comparison of different models' sample efficiency on the game "Pong". *DRL* deep reinforcement learning, *EDRL* episodic deep reinforcement learning, *MEDRL* modified episodic deep reinforcement learning

Table 3 Reward comparison of the different models on different games

Game	MEDRL	EDRL	Traditional DRL	Multi-MEDRL
Hero	13,533	8955.5	4868.7	13,627
Qbert	9538.2	5867.6	3885.3	9539.6
Pong	21	20.8	20.6	21

DRL deep reinforcement learning, *EDRL* episodic deep reinforcement learning, *MEDRL* modified episodic deep reinforcement learning, *Multi-MEDRL* multiple episodic memory deep reinforcement learning

stage) involved relatively simple treatment modalities and a short duration, and the total reward gap between the different models was small. In the second stage of the treatment process (the ROSC stage), the total reward gap between the different models was large.

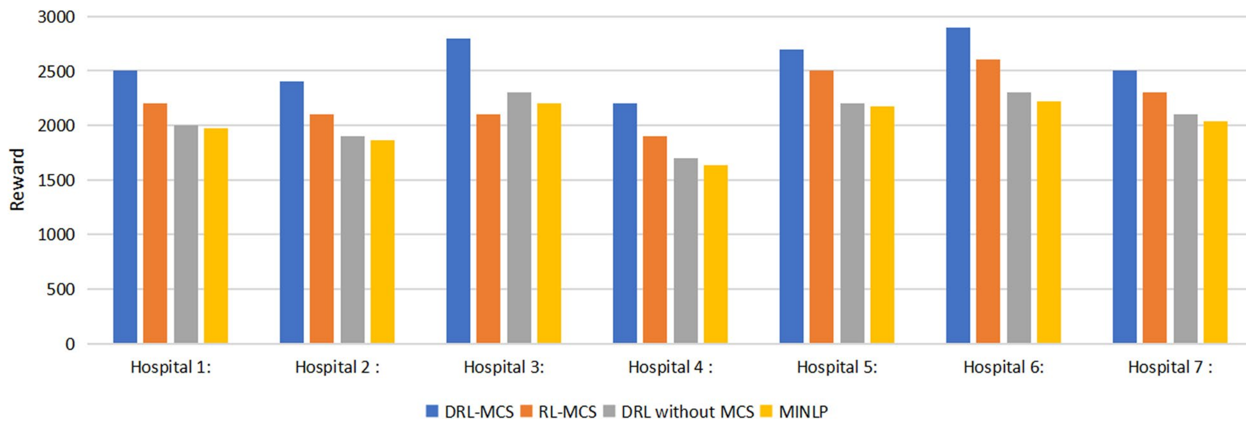

Fig. 6 Comparative results of the different models of stage 1. *DRL* deep reinforcement learning, *MCS* Monte Carlo simulation, *RL* reinforcement learning

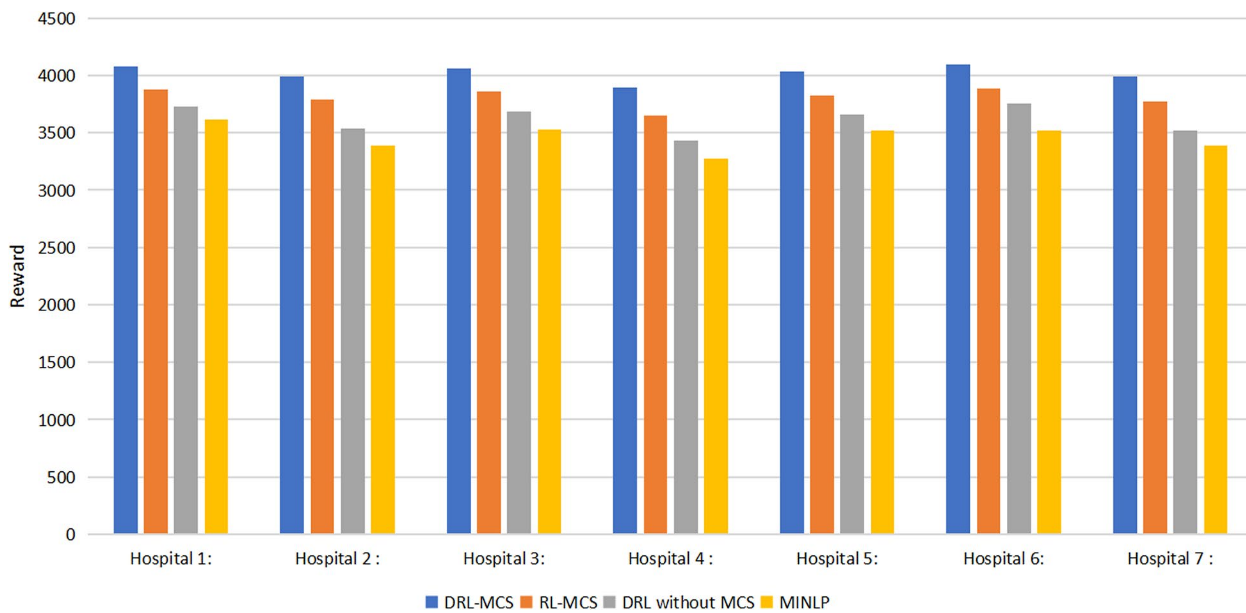

Fig. 7 Comparative results of the different models of stage 2. *DRL* deep reinforcement learning, *MCS* Monte Carlo simulation, *RL* reinforcement learning

In both the first and second stages, the proposed MEDRL-MCS-RVC model obtained a higher total reward, thereby achieving the best treatment effect. Although the MINLP is the one of the best physical models, it inevitably produces large scheduling errors and its permanence is the worst in both the first and second stages. Compared with the MINLP model, the MEDRL-MCS-RVC, MEDRL-MCS, and MEDRL-MCS models are all statistical models, which can get better results. Compared with using only MEDRL, uncertainty analysis can reduce errors during diagnosis and treatment. Moreover, RVC effectively implements uncertainty analysis by establishing dependencies between different basic parameters. Both factors effectively enhanced the accuracy of the treatment process. For further comparison of the performances of the three models, the mean and median values of the rewards of the seven hospitals are listed in Table 4, which shows that the DRL-MCS model proposed in this study achieved the best results.

Performance evaluation of HMTD

The HMTD is used to construct virtual samples to improve system performance when the original data are insufficient or basic patient information is missing. To

Table 4 Comparison of the three models at seven different hospitals

Hospital #	Model	Stage	Mean reward	Median reward
Hospital 1	MEDRL-MCS-RVC	**Stage 1**	2480	2500
		Stage 2	4080	4085
	MEDRL-MCS	**Stage 1**	2200	2100
		Stage 2	3880	3876
	MEDRL	**Stage 1**	1980	1900
		Stage 2	3730	3725
	Multi-MEDRL	**Stage 1**	2490	2507
		Stage 2	4123	4087
Hospital 2	MEDRL-MCS-RVC	**Stage 1**	2400	2300
		Stage 2	3980	3975
	MEDRL-MCS	**Stage 1**	2150	2100
		Stage 2	3782	3776
	MEDRL	**Stage 1**	2100	2000
		Stage 2	3536	3530
	Multi-MEDRL	**Stage 1**	2453	2379
		Stage 2	4087	4033
Hospital 3	MEDRL-MCS-RVC	**Stage 1**	2800	2800
		Stage 2	4055	4050
	MEDRL-MCS	**Stage 1**	2450	2500
		Stage 2	3860	3853
	MEDRL	**Stage 1**	2300	2200
		Stage 2	3687	3655
	Multi-MEDRL	**Stage 1**	2803	2809
		Stage 2	4107	4057
Hospital 4	MEDRL-MCS-RVC	**Stage 1**	2100	2200
		Stage 2	3896	3885
	MEDRL-MCS	**Stage 1**	1920	1900
		Stage 2	3655	3639
	MEDRL	**Stage 1**	1700	1600
		Stage 2	3420	3415
	Multi-MEDRL	**Stage 1**	1930	1952
		Stage 2	3698	3685
Hospital 5	MEDRL-MCS-RVC	**Stage 1**	2750	2700
		Stage 2	4025	4028
	MEDRL-MCS	**Stage 1**	2500	2500
		Stage 2	3810	3823
	MEDRL	**Stage 1**	2200	2100
		Stage 2	3657	3680
	Multi-MEDRL	**Stage 1**	2770	2695
		Stage 2	4050	4037
Hospital 6	MEDRL-MCS-RVC	**Stage 1**	2980	2900
		Stage 2	4096	4098
	MEDRL-MCS	**Stage 1**	2600	2500
		Stage 2	3886	3893
	MEDRL	**Stage 1**	2300	2300
		Stage 2	3753	3759
	Multi-MEDRL	**Stage 1**	3010	2980
		Stage 2	4107	4089
Hospital 7	MEDRL-MCS-RVC	**Stage 1**	2500	2500
		Stage 2	3990	3983
	MEDRL-MCS	**Stage 1**	2300	2200
		Stage 2	3770	3760
	MEDRL	**Stage 1**	2120	2200
		Stage 2	3523	3516
	Multi-MEDRL	**Stage 1**	2550	2530
		Stage 2	4010	3995

MCS, Monte Carlo simulation; MEDRL, modified episodic deep reinforcement learning; RVC, regular vine copula

verify the effectiveness of the proposed model (MEDRL-MCS-RVC-HMTD), we used three comparative models: MEDRL-MCS-RVC-multi distribution mega trend diffusion (MEDRL-MCS-RVC-MDMTD, MDMTD uses two types of distributions to describe the sample space), MEDRL-MCS-RVC-MTD (using traditional MTD as the virtual sample construction tool), and MEDRL-MCS-RVC (without the virtual sample construction tool).

Owing to the abrupt nature of IHCA occurrence, interventions must often be initiated before complete data are available, especially basic demographics (age, sex, and presence of an underlying disease) that are difficult to access over time. Therefore, the intelligent diagnosis and treatment system should be able to act based only on scant information. In this study, the basic information for Stage 1 included age, sex, IHCA causes, initial heart rhythm, and presence of an underlying disease; for Stage 2, these included age, sex, partial pressure of carbon dioxide, initial systolic pressure, initial body temperature, and presence of an underlying disease. Figures 6 and 7 and Table 4 show that all three models achieved the best results in Hospital 6. We considered Hospital 6 representative, comparing the rewards when there were only two, three, and four types of basic information in both stages. The comparative results are shown in Table 5.

Training a well-performing DRL model requires a large amount of original data. However, obtaining sufficient data to construct an accurate model is often challenging. Therefore, virtual samples need to be created. Moreover, using Hospital 6 as a representative case, we compared the rewards using 50% and 30% of the original data (Table 6).

Tables 5 and 6 show that, for both stages, the rewards of all models decreased with the number of missing information items and the percentage of total original data decreasing. Compared with the other three models,

Table 5 Comparison of the three models at Hospital 6 when basic information was incomplete

Number of missing information items	Model	Mean reward in Stage 1	Mean reward in Stage 2
1	MEDRL-MCS-RVC-HMTD	2930	4012
	MEDRL-MCS-RVC-MDMT	2765	3869
	MEDRL-MCS-RVC-MTD	2485	3755
	MEDRL-MCS-RVC	2123	3581
2	MEDRL-MCS-RVC-HMTD	2841	3907
	MEDRL-MCS-RVC-MDMTD	2632	3756
	MEDRL-MCS-RVC-MTD	2321	3583
	MEDRL-MCS-RVC	1933	3586
3	MEDRL-MCS-RVC-HMTD	2727	3785
	MEDRL-MCS-RVC-MDMT	2569	3652
	MEDRL-MCS-RVC-MTD	2116	3576
	MEDRL-MCS-RVC	1722	3359

HTMD hybrid megatrend diffusion, *MCS* Monte Carlo simulation, *MEDRL* modified episodic deep reinforcement learning, *RVC* regular vine copula, *MDMTD* multi distribution mega trend diffusion

Table 6 Comparison of the three models at Hospital 6 when original data were insufficient

Percentage of total original data	Model	Mean reward in Stage 1	Mean reward in Stage 2
100%	MEDRL-MCS-RVC-HMTD	3120	4205
	MEDRL-MCS-RVC-MDMT	3097	4176
	MEDRL-MCS-RVC-MTD	3072	4120
	MEDRL-MCS-RVC	2980	4096
50%	MEDRL-MCS-RVC-HMTD	2335	3306
	MEDRL-MCS-RVC-MDMT	2152	3127
	MEDRL-MCS-RVC-MTD	1932	2787
	MEDRL-MCS-RVC	1528	2303
30%	MEDRL-MCS-RVC-HMTD	2019	2637
	MEDRL-MCS-RVC-MDMT	1785	2366
	MEDRL-MCS-RVC-MTD	1659	1922
	MEDRL-MCS-RVC	1231	1502

HTMD hybrid megatrend diffusion, *MCS* Monte Carlo simulation, *MEDRL* modified episodic deep reinforcement learning, *RVC* regular vine copula, *MDMTD* multi distribution mega trend diffusion

the MEDRL-MCS-RVC model obtained the worst results because it does not have the virtual sample construction tool. The results of MEDRL-MCS-RVC-MDMTD were better than those of MCS-RVC-MTD because MDMTD uses two types of distributions to describe the sample space, which can achieve better performance than traditional MTD. The rewards of the MEDRL-MCS-RVC model proposed in this study were still acceptable, even in the absence of three different kinds of basic information or using only 30% of the original data.

Discussion

We developed an intelligent diagnosis and treatment system for IHCA to propose a reasonable diagnosis and treatment plan. Accurately analyzing and formulating a targeted treatment plan remains difficult owing to the numerous causes and complexity of IHCA [34]. Currently, the treatment process for IHCA mainly relies on the subjective experience of doctors, which can easily lead to misdiagnosis. Therefore, research on building an intelligent diagnosis and treatment system to assist doctors in effectively treating IHCA under various conditions remains important, especially when the original data were insufficient or basic patient information is missing. Although this intelligent diagnosis and treatment system was designed for IHCA, it can also be used for OHCA due to the similarity between the pathogenesis of these two types of CA.

Many studies have shown that the entire treatment process for IHCA should be divided into two steps (CPR and ROSC), and the specific treatment steps vary greatly according to the basic conditions of the patient (including age, sex, causes of IHCA, initial heart rhythm, body temperature, systolic pressure, and presence of an underlying disease) [2, 35]. We found that age, CPR start time, total CPR duration, chest compression start time, total chest compression time, airway management start time, airway management mode, time of first adrenaline dose administration, a single dose of adrenaline injection, number of adrenaline injections, electrical defibrillation start time, and frequency of electric defibrillation were the main factors influencing the success of CPR. In contrast, body temperature, systolic pressure, and respiratory conditions affected ROSC results. These results were consistent with those reported in the literature [36]. Based on the above analysis, an intelligent diagnosis and treatment system for IHCA was developed with the objective of maximizing the success rates of CPR and maintaining the blood pressure at an optimal value during ROSC to complete the corresponding two-step treatment process. Specifically, a novel HMTD was used to construct a virtual sample to improve the system performance with MEDRL as the core system module to finish the diagnosis and treatment process; the stochastic scenario was generated simultaneously using MCS-RVC.

Although AI elements have been widely used in the medical field, AI is only used to analyze, summarize, and discuss relevant data in studies pertaining to IHCA. This is, to our knowledge, the first study to build an intelligent diagnosis and treatment system for the therapeutic process of IHCA and to use DRL to complete the specific treatment process. Through comparative verification, our study showed that the system produced a positive therapeutic effect.

Nevertheless, the intelligent diagnosis and treatment system developed in this study is only a prototype with many imperfections. For example, as there are not sufficient IHCA statistics, the system is limited to CA in adults, whereas respiratory arrest and hemorrhagic, traumatic, and other presumed non-cardiac causes are not included. Comorbidities are also a significant aspect that should be considered. We plan to collect more comprehensive IHCA data to further improve the deficiencies of the intelligent diagnosis and treatment system in future research.

Conclusion

In this study, we aimed to combine AI technology and medical diagnosis to develop an intelligent diagnosis and treatment system to assist doctors in effectively completing IHCA treatment even when the original data were insufficient or basic patient information was missing. To the best of our knowledge, this is the first study to develop an intelligent diagnostic and treatment system for CA. Through simple modifications (e.g., parameter adjustment and collection of sufficient corresponding input data), the intelligent diagnosis and treatment system proposed here can also be used for potential risk prediction and early management of patients before the occurrence of IHCA. The main conclusions are summarized as follows:

1) The novel HMTD used to construct a virtual sample to improve the system performance when the original data were insufficient or basic patient information was missing showed that the performance of the system was acceptable even in the absence of three different types of basic information or when using only 30% of the original data.
2) The proposed MEDRL, as the core system module to finish the diagnosis and treatment process, improved the episodic memory updating manner and ERM, and may effectively promote sample efficiency and make DRL a practical reality.
3) A stochastic scenario was generated using MCS to analyze uncertainties, and RVC was used to construct the dependencies among all basic parameters. To the best of our knowledge, this is the first study that considers dependency in the uncertainty analysis of medical diagnoses.
4) Nevertheless, the intelligent diagnosis and treatment system developed in this study is only a prototype with many imperfections. For example, as there were insufficient IHCA statistics, the system was limited to CA in adults, whereas respiratory arrest and hemorrhagic, traumatic, and other presumed non-cardiac causes were not included. In future research, we plan to collect more comprehensive IHCA data to improve the deficiencies of intelligent diagnosis and treatment systems.

Abbreviations

AI	Artificial intelligence
CA	Cardiac arrest
IHCA	In-hospital cardiac arrest
OHCA	Out-hospital cardiac arrest
CPR	Cardiopulmonary resuscitation
DL	Deep learning
DRL	Deep reinforcement learning
RL	Reinforcement learning
ROSC	Restoration of spontaneous circulation
MCS	Monte Carlo simulation
HMTD	Hybrid mega trend diffusion
RVC	Regular vine copula
MEDRL	Modified episodic deep reinforcement learning
ERM	Experience replay memory
MPDF	Marginal probability density function
ETIC	Emergency technology innovation center

Acknowledgements
Not applicable.

Author contributions
YS contributed to the conceptualization, methodology and writing of the original draft. ZY supervised the work and was in charge of the project administration. YZ contributed to writing, review and edition, funding acquisition, and visualization. WC contributed to data curation and writing of the original draft. All authors read and approved the final manuscript.

Funding
This work was supported by the Hebei Provincial Science and Technology Department Science and Technology Special Project for Winter Olympics (20488803D) and the Hebei Provincial Department of Finance government Funded Clinical Medical Personnel Training Project (LS202104).

Availability of data and materials
The datasets used and/or analyzed during the current study are available from the corresponding author on reasonable request.

Declarations

Ethics approval and consent to participate
The study was approved by the China Hebei Emergency Technology Innovation Centre (ETIC), Hebei, China (reference number: 20221015). All patients provided written informed consent.

Consent for publication
Not applicable.

Competing interests
Authors declare no conflict of interest.

Received: 15 December 2023 Accepted: 21 October 2024
Published online: 04 November 2024

References

1. Granfeldt A, Holmberg MJ, Nolan JP, Soar J, Andersen LW, International Liaison Committee on Resuscitation (ILCOR) Advanced Life Support Task Force. Targeted temperature management in adult cardiac arrest: Systematic review and meta-analysis. Resuscitation. 2021;167:160–72. https://doi.org/10.1016/j.resuscitation.2021.08.040.
2. Andersen LW, Holmberg MJ, Berg KM, Donnino MW, Granfeldt A. In-hospital cardiac arrest: a review. JAMA. 2019;321:1200–10. https://doi.org/10.1001/jama.2019.1696.
3. Abrams D, MacLaren G, Lorusso R, Price S, Yannopoulos D, Vercaemst L, et al. Extracorporeal cardiopulmonary resuscitation in adults: evidence and implications. Intensive Care Med. 2022;48:1–15. https://doi.org/10.1007/s00134-021-06514-y.
4. Kumar KM. ECPR-extracorporeal cardiopulmonary resuscitation. Indian J Thorac Cardiovasc Surg. 2021;37:294–302. https://doi.org/10.1007/s12055-020-01072-2.
5. Girotra S, Chan PS, Bradley SM. Post-resuscitation care following out-of-hospital and in-hospital cardiac arrest. Heart. 2015;101:1943–9. https://doi.org/10.1136/heartjnl-2015-307450.
6. Gill R, Teitcher M, Ruland S. Neurologic complications of cardiac arrest. Handb Clin Neurol. 2021;177:193–209. https://doi.org/10.1016/B978-0-12-819814-8.00029-9.
7. Pourmand A, Hill B, Yamane D, Kuhl E. Approach to cardiopulmonary resuscitation induced consciousness, an emergency medicine perspective. Am J Emerg Med. 2019;37:751–6. https://doi.org/10.1016/j.ajem.2019.01.051.
8. McMullan J, Gerecht R, Bonomo J, Robb R, McNally B, Donnelly J, et al. Airway management and out-of-hospital cardiac arrest outcome in the CARES registry. Resuscitation. 2014;85:617–22. https://doi.org/10.1016/j.resuscitation.2014.02.007.
9. Hamet P, Tremblay J. Artificial intelligence in medicine. Metabolism. 2017;69S:S36-40. https://doi.org/10.1016/j.metabol.2017.01.011.
10. Zhong FS, Xing J, Li X, Liu X, Fu Z, Xiong Z, et al. Artificial intelligence in drug design. Sci China Life Sci. 2018;61:1191–204. https://doi.org/10.1007/s11427-018-9342-2.
11. Krittanawong C, Zhang H, Wang Z, Aydar M, Kitai T. Artificial intelligence in precision cardiovascular medicine. J Am Coll Cardiol. 2017;69:2657–64. https://doi.org/10.1016/j.jacc.2017.03.571.
12. Bhinder B, Gilvary C, Madhukar NS, Elemento O. Artificial intelligence in cancer research and precision medicine. Cancer Discov. 2021;11:900–15. https://doi.org/10.1158/2159-8290.CD-21-0090.
13. Isasi I, Irusta U, Aramendi E, Eftestøl T, Kramer-Johansen J, Wik L. Rhythm analysis during cardiopulmonary resuscitation using convolutional neural networks. Entropy (Basel). 2020;22:595. https://doi.org/10.3390/e22060595.
14. Hajeb-M A, Cascella M, Valentine M, Chon KH. Deep neural network approach for continuous ECG-based automated external defibrillator shock advisory system during cardiopulmonary resuscitation. J Am Heart Assoc. 2021;10: e019065.
15. Jerkeman M, Lundgren P, Omerovic E, Strömsöe A, Riva G, Hollenberg J, et al. Association between type of bystander cardiopulmonary resuscitation and survival in out-of-hospital cardiac arrest: a machine learning study. Resusc Plus. 2022;10: 100245. https://doi.org/10.1016/j.resplu.2022.100245.
16. Kawai Y, Okuda H, Kinoshita A, Yamamoto K, Miyazaki K, Takano K, et al. Visual assessment of interactions among resuscitation activity factors in out-of-hospital cardiopulmonary arrest using a machine learning model. PLoS ONE. 2022;17: e0273787. https://doi.org/10.1371/journal.pone.0273787.
17. Jekova I, Krasteva V. Optimization of end-to-end convolutional neural networks for analysis of out-of-hospital cardiac arrest rhythms during cardiopulmonary resuscitation. Sensors (Basel). 2021;21:4105. https://doi.org/10.3390/s21124105.
18. Pateria S, Subagdja B, Tan AH, Quek C. End-to-end hierarchical reinforcement learning with integrated subgoal discovery. IEEE Trans Neural Netw Learn Syst. 2022;33:7778–90. https://doi.org/10.1109/TNNLS.2021.3087733.
19. Singh A, Chiu WY, Manoharan SH, Romanov AM. Energy-efficient gait optimization of snake-like modular robots by using multiobjective reinforcement learning and a fuzzy inference system. IEEE Access. 2022;10:86624–35. https://doi.org/10.1109/ACCESS.2022.3195928.
20. Li D, Chang CC, Liu CW, Chen WC. A new approach for manufacturing forecast problems with insufficient data: the case of TFT-LCDs. J Intell Manuf. 2013;24:225–33. https://doi.org/10.1007/s10845-011-0577-6.
21. Dong WC, Sun H, Tan J, Li Z, Zhang J, Zhao YY. Short-term regional wind power forecasting for small datasets with input data correction, hybrid neural network, and error analysis. Energy Rep. 2021;7:7675–92. https://doi.org/10.1016/j.egyr.2021.11.021.
22. Yang HY, Wang T, Tan ZY, Yu Y. Sample-efficient deep reinforcement learning via balance sample. In: Proceedings of the 37th Youth Academic Annual Conference of Chinese Association of Automation (YAC); 2022. p. 890–5. https://doi.org/10.1109/YAC57282.2022.10023918.
23. Min BJ, Kim KJ. Learning to play visual doom using model-free episodic control. In: Proceedings of the IEEE Conference on Computational Intelligence and Games (CIG); 2017. p. 223–5. https://doi.org/10.1109/CIG.2017.8080439.
24. Nishio D, Yamane S. Faster deep Q-learning using neural episodic control. In: Proceedings of the 42nd Annual Computer Software and Applications Conference (COMPSAC) IEEE Publications; 2018. p. 486–91. https://doi.org/10.1109/COMPSAC.2018.00075.
25. Krishna AB, Abhyankar AR. Time-coupled day-ahead wind power scenario generation: a combined regular vine copula and variance reduction method. Energy. 2023;265: 126173. https://doi.org/10.1016/j.energy.2022.126173.
26. Huang C, Moraga C. A diffusion-neural-network for learning from small samples. Int J Approx Reason. 2004;35:137–61. https://doi.org/10.1016/j.ijar.2003.06.001.
27. Tufenkci S, Alagoz BB, Kavuran G, Yeroglu C, Herencsar N, Mahata S. A theoretical demonstration for reinforcement learning of Pi control dynamics for optimal speed control of Dc motors by using Twin Delay Deep Deterministic Policy Gradient Algorithm. Expert Syst Appl. 2023;213: 119192. https://doi.org/10.1016/j.eswa.2022.119192.
28. Haq EU, Lyu C, Xie P, Yan S, Ahmad F, Jia Y. Implementation of home energy management system based on reinforcement learning. Energy Rep. 2022;8:560–6. https://doi.org/10.1016/j.egyr.2021.11.170.
29. Zhen S, Jirutitijaroen P. Latin hypercube sampling techniques for power systems reliability analysis with renewable energy sources. IEEE Trans Power Syst. 2011;26:2066–73. https://doi.org/10.1109/TPWRS.2011.2113380.
30. Zhang S, Cheng H, Zhang L, Bazargan M, Yao L. Probabilistic evaluation of available load supply capability for distribution system. IEEE Trans Power Syst. 2013;28:3215–25. https://doi.org/10.1109/TPWRS.2013.2245924.
31. Zhou C, Ban H, Zhang J, Li Q, Zhang Y. Gaussian mixture variational autoencoder for semi-supervised topic modeling. IEEE Access. 2020;8:106843–54. https://doi.org/10.1109/ACCESS.2020.3001184.
32. Wang Z, Wang W, Liu CC, Wang B. Forecasted scenarios of regional wind farms based on regular vine copulas. J Mod Power Syst Clean Energy. 2020;8:77–85. https://doi.org/10.35833/MPCE.2017.000570.
33. Yang D, Qin X, Xu X, Li C, Wei G. Sample efficient reinforcement learning method via high efficient episodic memory. IEEE Access. 2020;8:129274–84. https://doi.org/10.1109/ACCESS.2020.3009329.
34. Buckler DG, Burke RV, Naim MY, MacPherson A, Bradley RN, Abella BS, et al. Association of mechanical cardiopulmonary resuscitation device use with cardiac arrest outcomes: a population-based study using the CARES registry (cardiac arrest registry to enhance survival). Circulation. 2016;134:2131–3. https://doi.org/10.1161/CIRCULATIONAHA.116.026053.
35. Holmberg MJ, Granfeldt A, Moskowitz A, Andersen LW, American Heart Association's Get with The Guidelines-Resuscitation Investigators. Age-related cognitive bias in in-hospital cardiac arrest. Resuscitation. 2021;162:43–6. https://doi.org/10.1016/j.resuscitation.2021.01.016.
36. Merchant RM, Topjian AA, Panchal AR, Cheng A, Aziz K, Berg KM, et al. Part 1: Executive Summary: 2020 American Heart Association Guidelines for Cardiopulmonary Resuscitation and Emergency Cardiovascular Care. Circulation. 2020;142:S337–57. https://doi.org/10.1161/CIR.0000000000000918.

Publisher's Note